A Simulation Approach to Analyse the Impacts of Battery Swap Stations for e-Motorcycles in Africa

Cameron S Sheehan
Department of Electrical and Electronic Engineering
Imperial College London
London, United Kingdom
E-mail: cameron.sheehan19@imperial.ac.uk

Tim C Green
Department of Electrical and Electronic Engineering
Imperial College London
London, United Kingdom
E-mail: t.green@imperial.ac.uk

Nicolò Daina
Department of Civil and Environmental Engineering
Imperial College London
London, United Kingdom
E-mail: n.daina@imperial.ac.uk

***Abstract*—The recent rapid growth in the use of motorcycle taxis in many African countries has led to an increase in negative environmental impacts, such as local air pollution and carbon-emissions. Electrification of these motorcycles has been proposed as a solution to these issues and several pilot-projects are under way. However, the electricity systems in many of these countries are strained, with generation and/or distribution capacity at their limits, leading to regular power outages that could impact the charging of these e-motorcycles. These fragile grids may be put under further strain by additional e-motorcycle charging. Usage patterns of these commercial motorcycle taxis imply that drivers may not be willing to wait for extended periods to charge during their shift. The use of battery swapping stations could mitigate these issues, however, modelling of their system impacts is required to fully understand their potential. This paper presents a hybrid model to simulate the key operational processes of battery swapping stations and their energy systems, allowing various configurations and scenarios to be investigated for the specific context of e-motorcycles in Africa. The configuration parameters include the numbers of batteries and charging slots, the charging power, and the addition of solar PV and static battery energy storage capacity. Power outages can be modelled for various scenarios. A test case of a battery swap station in Nairobi, Kenya, was used to showcase and validate the model.**

***Index Terms*—battery swapping station model, energy system model, electric motorcycle, solar PV, battery energy storage, power outages, Nairobi Kenya, Africa**

I. Introduction

Expanding access to transport services is an important component of the economic development and growth in any country, as it is a means of providing access to healthcare, education and employment opportunities to its people. However, in many African countries, access to transport has been limited due to a number of factors, such as a lack of organised public transport infrastructure and the poor condition of roads [1].

These factors have contributed to the emergence and rapid growth of commercial motorcycle taxis in some African countries [1]. While these vehicles are helping to increase access to transport, they are also responsible for a number of negative environmental impacts, such as increasing carbon-emissions and local air pollution [2].

Electrification of these motorcycles has been proposed as a solution to these issues, with a number of pilot-projects currently under way, and the Government of Rwanda planning to release policy that will no longer permit non-electric motorcycles into their fleet [3]. Electric motorcycles (e-motorcycles or EMs) produce no local air pollution, and have the potential to reduce carbon-emissions, though this is dependent on the electricity mix in the country. The charging of these vehicles in many African countries could be impacted by their strained electricity systems, with generation and/or distribution capacity at their limits, leading to regular power outages [4]. These fragile grids may also be put under further pressure by these additional charging loads. This means their grids may not be able to support the charging of these e-motorcycles and could present major barriers to their deployment in these countries. Furthermore, the usage patterns of these motorcycle taxis imply that drivers may not be willing to wait for extended periods of time to charge during their shift [5].

Battery swapping stations (BSSs) are an option that could overcome some of these issues, and feature in some pilot-projects [6], [7]. Battery swapping is a convenient method for circumventing the issue of waiting for a battery to charge before being able to travel again since the swapping of a discharged battery for a fully charged one occurs in a relatively short time at a BSS [8]. Battery swapping is also particularly suited to motorcycles since they generally require smaller batteries, which are easier to remove and handle during swapping [8]. A recent paper on energy and transport in Africa and South Asia [9] identified key knowledge gaps that lie at the intersection between mobility and power systems, and specifically around determining the impacts of EM BSSs on the power generation and distribution networks in these regions.

A. Related Work

BSSs, along with their energy systems, have been studied in the literature to varying extents and for different purposes. For instance, reference [10] used the HOMER Pro simulation software to investigate using BSSs for electric rickshaws in Bangladesh as a distributed energy source to allow integration of intermittent renewable energy sources. The study assumed a number of naturally stochastic variables (e.g. battery state of charge (SOC), number of swaps per vehicle and time of charging) to be constant which may reduce the practicality of

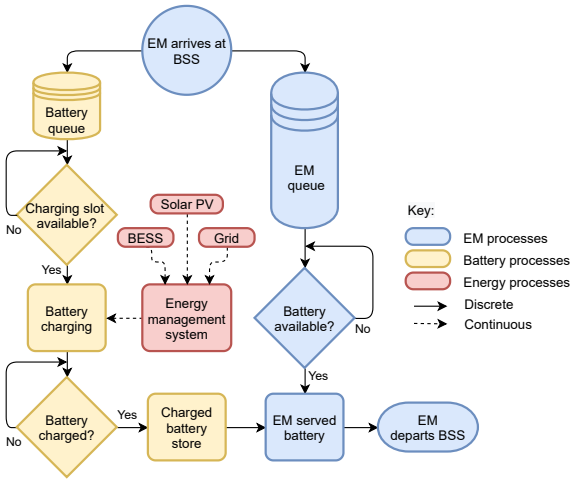

Fig. 1. Flow diagram of Battery Swap Station Model. Source: Author adapted from [13].

certain results. Whereas the authors of [11] take the random values of SOC, charging time and vehicle arrivals into consideration in their queuing network model of a BSS. Similarly, in [12], a stochastic model was proposed to investigate the operation of BSSs for buses and taxis.

While these and other models have their merits, no single comprehensive model was found in literature that could take into account the various aspects of BSSs for the specific context of EMs in Africa.

B. Our Contributions

The dearth of available data on EM usage in African Cities due to their recent introduction is a significant challenge in impact studies of EM deployment. To address this challenge, we adopted a simulation approach to analyse how different configurations of BSSs perform under various scenarios and what their potential benefits and impacts may be. Our model was developed to be comprehensive and sensitive to factors that are specific to the context of battery swap stations for EMs in African cities. These factors include the stochastic nature of various battery swap demand inputs, the integration of solar photovoltaic (PV) and battery energy storage systems (BESSs), the system response to grid power outages, and their impacts on the grid load.

II. Model Design and Methods

The key processes involved in the model are summarised in the simplified flow diagram of the BSS shown in Fig. 1. This diagram has been adapted from [13]. It shows that the model comprises three broad categories of processes:

a) EM taxi processes: These involve the EM taxi which is modelled as a discrete entity that arrives at the BSS, drops off its battery, waits in a queue until a battery is available, then is served a battery before departing from the station.

b) Battery processes: These involve the swappable battery which is also modelled as a discrete entity that arrives at the BSS with the EM taxi, waits in a queue until a charging slot is available, undergoes charging, and is then stored at the BSS until it is served to an EM taxi.

c) Power and energy processes: These involve continuous time based signals that represent either power or energy flow between the different energy sources (grid, solar PV, and battery energy storage system (BESS)) and the batteries being charged at the charging slots. An energy management system is used to control the dispatch of energy between these different sources.

A. Development Environment

To realise and implement these models, the MATLAB software along with the add-on packages, Simulink and SimEvents, were used. The interface between Simulink and SimEvents allows for the creation of time and events-based hybrid models [14], which allowed the BSS discrete event processes and the continuous time based power and energy components of the model to be connected and function as a single hybrid model of the BSS.

B. Inputs and Data Pre-processing

The various inputs and any pre-processing that was performed on the data are detailed below.

1) Batteries arriving at the BSS: The model uses probabilities of arriving EM taxis at the BSS for each 30 minute period of the simulated day, as well as the distribution of battery SOC's during each time period as inputs.

a) Arrival rates: The normalised probability of battery swap events, $P_{swap,i}$, occurring in each 30 minute time period, i, is first used to create a distribution of average arrival rates of the EM taxis at the BSS, $\lambda_{swap,i}$ (*taxis arriving/time period*), for each time period of the simulated day. This can be calculated as shown below in (1).

$$\lambda_{swap,i} = \frac{P_{swap,i} \cdot N_{EM} \cdot N_{swaps/EM/day}}{\Delta t_{period}} \tag{1}$$

Where Δt_{period} is the length of each time period (30 minutes), N_{EM} is the number of EM taxis being simulated, and $N_{swaps/EM/day}$ is the number of battery swaps per EM taxi per day, as output from the EM taxi model.

The model assumed that the arrivals of the batteries corresponded with a Poisson arrival process [15], such that the interarrival times of the arriving entities (EM taxis) could be calculated using (2) adapted from [16].

$$dt = -\frac{1}{\lambda_{swap,i}} \cdot \log(1 - R) \tag{2}$$

Where R is a random number in the range 0 to 1.

b) Battery SOC upon arrival: The SOC of the i^{th} battery arriving at the station, $SOC_{batt.arrive.i}$, is drawn from a gamma distribution configured with the mean and standard deviation of the SOC in that time period.

2) Solar irradiance: The model allows daily solar irradiation data (kWh/m^2) to be input in 15 minute intervals.

3) Other transformer load: In order to investigate the affect of the BSS load on the grid, a scale-able load profile for the region of interest was required. The model allows a transformer load rating to be input as a means of scaling the other load profile at the distribution transformer for the simulations. A load profile for Nairobi was input from [17].

4) Power outages: In order to investigate the effect of power outages on the performance of the BSS, key metrics for these outages were required. The average duration of the outages and the average number of outages experienced per month (outage frequency) were used as inputs as they are available for most regions. For Nairobi, these values were 5.8 and 3.8 respectively [4]. For the timing of these outages, data was found for Nairobi that showed that outages occurred most frequently at 09:00 (morning) and 19:00 (evening) [18], coinciding with morning and evening peak load periods.

C. Configuration Parameters and Sizing of Components

The model was setup such that a range of different BSS design configurations could be simulated. For convenient scaling of these results to different numbers of EM taxis, the number of BSS batteries and BSS charging slots were input as ratios per vehicle. Similarly, the solar PV and BESS capacities were input as ratios relative to the station's capacity and backup supply requirements, respectively. These parameters are discussed in further detail below.

1) Number of BSS batteries and charging slots: The number of BSS batteries and charging slots in the simulation, $N_{batt.}$ and $N_{ch.sl}$, were input by varying the ratio of batteries and charging slots per EM. These ratios shall be referred to as the BSS battery ratio, BR, and BSS charge slot ratio, CSR, respectively, and are formally defined in (3) and (4).

$$BR = \frac{N_{batt.}}{N_{EM}} \tag{3}$$

$$CSR = \frac{N_{ch.sl}}{N_{EM}} \tag{4}$$

Where N_{EM} is the total number of EMs considered.

2) Power of BSS chargers: The model allows the power ratings of the BSS charging slots, $W_{ch.sl}$ (kW), to be input as discrete values.

3) BSS charging capacity: Once the number of BSS charge slots and their power rating have been set, the BSS total charging capacity, $W_{BSS.ch}$ (kW), can be calculated using (5).

$$W_{BSS.ch} = N_{ch.sl} \cdot W_{ch.sl} \tag{5}$$

This value is useful in determining the solar PV and BESS capacities.

4) Solar PV capacity: The installed solar PV capacity at the BSS, W_{PV} (kWp), was input by varying the ratio of PV capacity to the BSS charging capacity. This ratio shall be referred to as the BSS PV Capacity Ratio, PVR, and is formally defined in (6).

$$PVR = \frac{W_{PV} \cdot \eta_{inv}}{W_{BSS.ch}} \tag{6}$$

Note that since the PV current would be converted from DC to AC using an inverter (discussed in further detail in Section II-C6), the inverter's efficiency, η_{inv}, was taken into account when calculating the PVR.

5) BESS capacity: The battery energy storage system (BESS) was sized according to the ability to serve as a backup power supply for the BSS during power outages. The BESS discharge power capacity, W_{BESS} (kW), was calculated using (7).

$$W_{BESS} = \frac{W_{BSS.ch}}{\eta_{inv}} \tag{7}$$

The BESS energy capacity, E_{BESS} (kWh), was calculated based on supplying the maximum discharge power for a portion of the mean length of the power outage, $\mu_{outage.length}$ (hr), as well as taking into account the maximum depth of discharge, DOD_{BESS}, as shown in (8).

$$E_{BESS} = BESR \cdot \frac{\mu_{outage.length} \cdot W_{BESS}}{DOD_{BESS}} \tag{8}$$

Therefore, the BESS energy capacity ratio, $BESR$, can be formally defined in (9).

$$BESR = \frac{E_{BESS} \cdot DOD_{BESS}}{\mu_{outage.length} \cdot W_{BESS}} \tag{9}$$

The model was setup such that the BESS only supplied power during outages, and was not used to supplement the BSS charging load outside of these outage periods.

6) Inverter capacity: The configuration of the BSS considered in this model is AC coupled. Therefore, both the PV and BESS require inverters to convert from DC to AC. The capacity of the inverters were sized according to (10), adapted from [19].

$$W_{inv.} = SF_{inv.} \cdot (W_{PV} + W_{BESS}) \tag{10}$$

Where $SF_{inv.}$ is the safety factor included for the inverter power rating. A value of 1.3 was used in this model [19].

D. Power and Energy Dispatch

To model the different energy sources and charging of the batteries at the BSS, the power and energy dispatch of each source was modelled. The mathematical formulation that forms the basis of the Simulink block diagrams in the model shall be detailed in this section. A simplified diagram showing the configuration of the station with all possible energy sources is shown in Fig. 2. Details of the models for each power source are provided in the following sections.

1) Power from solar PV: Based on the installed PV capacity at the BSS, W_{PV}, and specifications for the solar PV modules, the total area of solar PV, A_{PV} (m^2), could be calculated using (11).

$$A_{PV} = \frac{W_{PV} \cdot A_{panel}}{W_{panel}} \tag{11}$$

Where A_{panel} is the area of a single solar PV panel (m^2), and W_{panel} is the panel's peak power rating (kW_p).

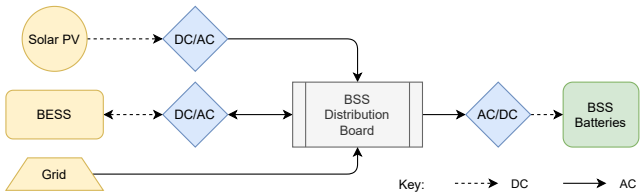

Fig. 2. Simplified diagram of BSS configuration with all energy sources.

Using the irradiance data input discussed in Section II-B2, $I_{solar}(t)$ (kW/m^2), and the installed PV area at the BSS, A_{PV}, the power output from the solar PV, $w_{PV}(t)$ (kW), could be calculated using (12), adapted from [19]:

$$w_{PV}(t) = I_{solar}(t) \cdot A_{PV} \cdot \eta_{PV} \cdot \eta_{inv} \quad (12)$$

Where η_{PV} is the efficiency of the PV modules, and η_{inv} is the efficiency of the DC to AC inverter.

2) Battery energy storage system discharging power and charging load: The lead-acid BESS was modelled to be a back-up power supply at the BSS. Since a BESS is a storage device, and not a generation source, it involves both charging and discharging processes. The modelling of these processes is detailed below.

a) BESS discharging: For discharging the BESS to supply charging load at the BSS, the following assumptions were made to model the discharge power, $w_{BESS}(t)$ (kW):

- The BESS was modelled to only discharge during power outages.
- The BESS would only discharge the remaining charging load not met by the installed PV.
- The discharge power was limited to the BESS discharge power capacity, W_{BESS}, as set in Section II-C.
- The BESS was modelled to have a maximum depth of discharge, DOD_{BESS}, of 60% [20]. Therefore, the BESS would not discharge if the SOC, $SOC_{BESS}(t)$, fell below 40%, i.e. $SOC_{BESS.min} = 0.4$.

b) BESS charging: For charging the BESS, the following assumptions were made to model the charging load from the grid, $w_{BESS.grid.ch}$ (kW), and charging load from PV, $w_{BESS.PV.ch}$ (kW).

- Charging from the grid was assumed to only occur during off-peak periods between 0:00 and 06:00.
- The charging rate was set to 0.2C [21] (i.e. $w_{BESS.grid.ch}(t) = 0.2 \times W_{BESS}$).
- If no PV was installed, the charging of the BESS would occur from the grid only, and the maximum SOC of the BESS, $SOC_{BESS.grid.max}$, was set to 100%
- If PV was installed, the grid would only charge up to a maximum, $SOC_{BESS.grid.max}$, of 80%, resulting in 20% available to charge from excess PV power the following day.
- If excess PV power was generated after supplying the BSS charging load, then this excess power, $w_{BESS.PV.ch}(t)$, would be used to charge the BESS.

3) BSS charging slots load: In periods where outages were not occurring, the total charging slots load was calculated based on the BSS charge slot power rating, $W_{ch.sl}$, and the number of BSS charge slots in use, $n_{ch.sl}(t)$, as per (13).

$$w_{BSS}(t) = W_{ch.sl} \cdot n_{ch.sl}(t) \quad (13)$$

However, if an outage was occurring, then the charging load was limited to the maximum power supplied by PV and/or BESS, as per (14).

$$w_{BSS}(t) = min[W_{ch.sl} \cdot n_{ch.sl}(t); w_{PV}(t) + w_{BESS}(t)] \quad (14)$$

The SOC of the batteries that arrived at the BSS, $SOC_{batt.ar.i}(t)$, were used to determine the amount of energy in the batteries, $E_{batt.ar.i}$(t), at the beginning of charging when they are assigned to the charging slots, according to (15).

$$E_{batt.ar.i} = SOC_{batt.ar.i} \cdot E_{batt.cap} \quad (15)$$

Where $E_{batt.cap}$ is the assumed battery energy capacity of the batteries used in the simulation (3 kWh).

The energy in the battery was then updated throughout the charging process using (16).

$$E_{batt.i}(t) = E_{batt.ar.i} + \frac{\eta_{ch.}\eta_{batt.rt}}{60} \int_{t.st.ch}^{t} \frac{w_{BSS}(t)}{n_{ch.sl}(t)} dt \quad (16)$$

Where $\eta_{batt.rt}$ is the round-trip efficiency of the battery and $\eta_{ch.}$ is the charger efficiency. Note that the simulation time unit was in minutes, therefore, to convert to kWh the factor of 1/60 was included. The efficiency of the charging process is assumed to be constant in the model.

The charging slot was modelled to release the battery when it reached an SOC of 100% (i.e. when $E_{batt.i}(t) = E_{batt.cap}$). After which, the charging slot would be available to be assigned the next battery in the queue.

4) BSS load on grid: The load of the BSS on the grid, $w_{grid}(t)$ (kW), was modelled to be the difference between the BSS charging load, $w_{BSS}(t)$, and the power supplied by solar PV, $w_{PV}(t)$, with the addition of the possible load from recharging the BESS, $w_{BESS.ch}(t)$. However, if an outage was set to occur, the grid load was set to zero.

III. Case Study and Discussion

The city of Nairobi, Kenya, was chosen as a case study location for inputs to validate the model. For the purpose of checking the different sub-components of the model and their interaction with each other, a BSS configuration was chosen such that it could demonstrate all of their interactions in a single simulation. Through a series of trial runs, the following configuration inputs for Nairobi were found to demonstrate all the required results for model validation:

BSS battery ratio, $BR = 1.4$
BSS charge slot ratio, $CSR = 0.14$
BSS charge slot power rating, $W_{ch.slots} = 2.0\ kW$

BSS PV capacity ratio, $PVR = 1.5$
BESS energy capacity ratio, $BESR = 0.5$

Note that in order to validate that the queuing model was functioning, the station was configured to be sub-optimal in terms of service delivery, such that a queue of EMs waiting for charged batteries built up at the station and could be checked.

The simulation was run for 100 EM taxis over 4 days using a 4-day irradiance profile from [22]. Typical evening and morning power outages were simulated on the first and fourth days (highlighted in red), each lasting 5.8 hours [4]. The results for the Nairobi simulation are shown in Fig. 3.

A. EM Taxi Arrivals and Queuing at the BSS

The number of EM taxi arrivals at the BSS per 30 minute period, as well as the EM taxi queue at the BSS, for the simulation are shown in Fig. 3a. As shown, the Poisson arrival process has created distributions of EM taxi arrivals for battery swaps throughout each day, with peaks in arrivals during the morning, lunch and early evening periods corresponding with the sample of average arrival rates used as an input for the model. It can also be seen that the arrival distributions vary by day due to the Poisson process, which provides randomness to the model. A queue starts to build up at approximately 15:00 on the first day, and reaches a maximum of 13 EMs at around 21:00. The queue then remains constant from 22:00 since no more arrivals happen, and no batteries are being charged and dispensed to the EMs due to the power outage. As seen at hour 26, the queue rapidly drops to zero since the batteries that were charging after the outage reach the fully charged state and are dispensed to the EMs. Note that the station configuration for this simulation results in a total of 14 BSS charge slots, so the queue of 12 EMs after the outage are able to be served in one go once the batteries were released. A queue can also be seen to build up on the second day and third days to a maximum of five and two EMs respectively. These different queues imply that the station has a sub-optimal configuration (as was chosen for this validation simulation).

B. Power and Energy Dispatch

The different charging and load profiles at the simulated BSS and substation are depicted in Fig. 3b and Fig. 3c, while the SOC of the BESS throughout the simulation is shown in Fig. 3d. As seen in Fig. 3c, the other load at the substation (blue) is scaled from the input discussed in Section II-B, with the outages resulting in no grid load during those periods. Since the first outage occurs in the evening, there is only BESS available to supply the BSS charging loads. Fig. 3c shows this configuration would increase the evening peak load at the transformer by approximately 20%.

Recalling that the $BESR$ was set to a ratio of 0.5 for this simulation configuration, it can be seen in Fig. 3b that the BESS is only able to supply the load for half of the outage period. Fig. 3d, shows the SOC of the BESS drop to the minimum set value, $SOC_{BESS.min}$, of 40%, after which it stops discharging and the SOC remains constant. After the first grid outage is over, the BESS starts to recharge from the grid at a slower charging rate (0.2C) until 06:00 (hr 30) the following morning.

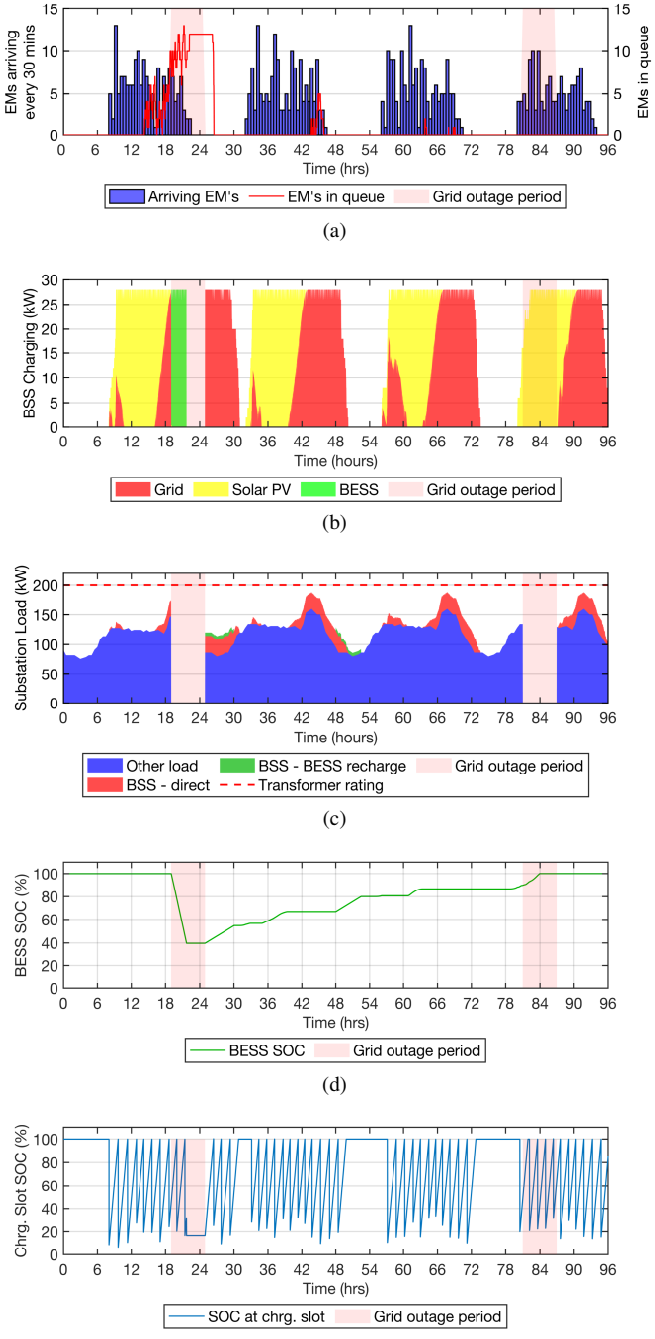

Fig. 3. Results from the 4-day (96 hour) Nairobi BSS simulation for (a) EM taxi arrivals and queue at BSS, (b) BSS charging load profiles, (c) substation load profiles, (d) BESS SOC, and (e) SOC of batteries at a BSS charge slot.

During periods of excess PV power (see hrs 32-33, 35-39, 56-63 and 79-84), where the BSS charging load on the grid reduces to zero, Fig. 3d shows that the model recharges the BESS with this excess energy. Since the maximum SOC for the BESS to be charged from the grid, $SOC_{BESS.grid.max}$, was set to 80%, it can be seen that the BESS is not charged

overnight on the third evening since the SOC is above this level. The SOC of the BESS then gets charged to its maximum of 100% on the fourth day by excess PV power. The BSS charging load during the outage on the fourth day was fully supplied by the PV power, and so no BESS power was discharged. As shown by these various processes, the model of the energy system was correctly functioning inline with the set control algorithms.

C. Charging of Batteries at the BSS

To validate whether the individual charging slots at the BSS were functioning as intended, the SOC of the batteries at one of the charging slots at the BSS was sampled with results shown in Fig. 3e. Note that the signal indicating the SOC of the battery at a slot indicates 100% when the slot is empty. When a battery is assigned to the charge slot, the SOC of the arriving swap battery is reflected by the sudden drop of the SOC at the charging slot and rises at the rate set by the charging power until the battery reaches 100% SOC. The charged battery is then released to the BSS battery store, and a new battery is assigned to the charger and the process starts again. Halfway through the first outage, where the BESS stopped discharging, it can be seen that the SOC of the battery at the charge slot remains constant until the outage is over following which, charging resumes.

IV. Conclusions

With the increasing use of electric motorcycles in Africa to combat emissions and pollution from conventional ICE motorcycles, an understanding of the charging infrastructure and its impact on weak grid systems is very important. A model was developed to capture the key operational process of a battery swapping station and its energy system which allows various station configurations to be investigated. These configurations include the numbers of batteries and charging slots, the charging power, and the addition of solar PV and battery energy storage capacity. The impact of power outages on battery swapping can be modelled for various scenarios. A case study was presented for a BSS configuration in Nairobi. The results demonstrated how the various sub-models performed and interacted with each other, and clearly showed what impact the chosen BSS configuration would have on the grid in terms of charging load. This simulation model can be used as an analysis tool when planning new BSSs for e-motorcycles in African cities and can show the potential impacts and benefits of various configurations.

Acknowledgment

This paper is based on work reported in the first author's MSc thesis [23]. The authors would like to thank Alec Edwards for his previous unpublished work in this area [13].

References

[1] A. Kumar, "Understanding the emerging role of motorcycles in African cities: A political economy perspective," Sub-Saharan Africa Transport Policy Program, Tech. Rep., 2011.

[2] D. Ehebrecht, D. Heinrichs, and B. Lenz, "Motorcycle-taxis in sub-Saharan Africa: Current knowledge, implications for the debate on "informal" transport and research needs," *Journal of Transport Geography*, vol. 69, no. May 2018, pp. 242–256, 2018.

[3] J. Bright, "Rwanda to phase out gas motorcycle taxis for e-motos," 2019. [Online]. Available: https://techcrunch.com/2019/08/28/rwanda-to-phase-out-gas-motorcycle-taxis-for-e-motos/

[4] The World Bank, "Kenya: Infrastructure," 2018. [Online]. Available: https://www.enterprisesurveys.org/en/data/exploreeconomies/2018/kenya#infrastructure

[5] J. de la Croix Tabaro, "New Electric Motorcycle Hits Rwandan Roads Next Month," 2019. [Online]. Available: https://www.ktpress.rw/2019/10/new-electric-motorcycle-hits-rwandan-roads-next-month/

[6] Ampersand, "Ampersand," 2020. [Online]. Available: https://ampersand.solar/

[7] MAXOkada, "Exploring Future Power, Disrupting Mobility! - MAXOkada - Medium," 2019. [Online]. Available: https://medium.com/@MAXOkada/exploring-future-power-disrupting-mobility-2bee31166df5

[8] C. Chen and G. Hua, "A New Model for Optimal Deployment of Electric Vehicle Charging and Battery Swapping Stations," *International Journal of Control and Automation*, vol. 7, no. 5, pp. 247–258, 2014.

[9] K. A. Collett, M. Byamukama, C. Crozier, and M. Mcculloch, "Energy and Transport in Africa and South Asia: State of knowledge paper," Energy and Economic Growth: Applied Research Programme, Tech. Rep., 2020.

[10] A. S. M. M. Hasan, "Electric Rickshaw Charging Stations as Distributed Energy Storages for Integrating Intermittent Renewable Energy Sources: A Case of Bangladesh," *Energies*, vol. 13, no. 6119, pp. 1–28, 2020.

[11] B. Sun, X. Tan, and D. H. K. Tsang, "Optimal charging operation of battery swapping stations with QoS guarantee," in *2014 IEEE International Conference on Smart Grid Communications (SmartGridComm)*. IEEE, 11 2014, pp. 13–18.

[12] T. Zhang, X. Chen, Z. Yu, X. Zhu, and D. Shi, "A Monte Carlo Simulation Approach to Evaluate Service Capacities of EV Charging and Battery Swapping Stations," *IEEE Transactions on Industrial Informatics*, vol. 14, no. 9, pp. 3914–3923, 9 2018.

[13] A. Edwards and T. Green, "Energy for Development: Electric Traction - Electrification of Small Commercial Vehicles in Urban Areas Across Sub-Saharan Africa," 2019, Energy Futures Lab, Imperial College London, unpublished.

[14] M. I. Clune, P. J. Mosterman, and C. G. Cassandras, "Discrete Event and Hybrid System Simulation with SimEvents," in *Eighth International Workshop on Discrete Event Systems, WODES 2006*. Ann Arbor, MI, USA: IEEE, 2006, pp. 386–387.

[15] B. Sun, X. Sun, D. H. Tsang, and W. Whitt, "Optimal battery purchasing and charging strategy at electric vehicle battery swap stations," *European Journal of Operational Research*, vol. 279, no. 2, pp. 524–539, 12 2019.

[16] MathWorks, "Model Traffic Intersections as a Queuing Network - MATLAB & Simulink," 2020. [Online]. Available: https://www.mathworks.com/help/simevents/ug/generate-random-numbers-in-simevents.html

[17] Lahmeyer International GmbH, "Development of a Power Generation and Transmission Master Plan, Kenya: Medium Term Plan 2015-2020 Volume II - Annexes," Lahmeyer International GmbH, Tech. Rep., 2016.

[18] J. Taneja, "Measuring Electricity Reliability in Kenya," STIMA Lab, Dept. of Elec. and Comp. Eng., University of Massachusetts, Tech. Rep., 2016.

[19] A. Siriwattanapong and C. Chantharasenawong, "Electric motorcycle charging station powered by solar energy," *IOP Conference Series: Materials Science and Engineering*, vol. 297, no. 1, 2018.

[20] E. Lockhart, X. Li, S. Booth, J. Salasovich, D. Olis, J. Elsworth, and L. Lisell, "Comparitive Study of Techno-Economics of Lithium-Ion and Lead Acid Batteries in Micro-Grids in Sub-Saharan Africa," National Renewable Energy Laboratory (NREL), Tech. Rep., 2019.

[21] O. Veneri, C. Capasso, and D. Iannuzzi, "Experimental evaluation of DC charging architecture for fully-electrified low-power two-wheeler," *Applied Energy*, vol. 162, pp. 1428–1438, 1 2016.

[22] SoDa Service, "HelioClim-3 Archives demo," 2020. [Online]. Available: http://www.soda-pro.com/web-services/radiation/helioclim-3-archives-for-free

[23] C. S. Sheehan, "Enabling e-Mobility in Africa: A Techno-Economic Study of Battery Swap Options for e-Motorcycle Taxis," Master's thesis, Imperial College London, London, 2020.